*Desalination and Water Treatment*
www.deswater.com

doi: 10.5004/dwt.2019.23829

151 (2019) 384–391
May

# Adsorption characteristics of tetracycline on biochar from agricultural wastes

Yingjie Dai[a,b], Mei Liu[c], Yue Sun[b], Jingjing Li[b], Yue Jiang[d], Shanshan Li[b], Wu Yue[b], Zhihua Liu[b,*]

[a]*Key Laboratory of Original Agro-Environmental Pollution Prevention and Control, Ministry of Agriculture/Tianjin Key Laboratory of Agro-environment and Safe-product,No.31 Fukang Road, Nankai District, Tianjin 300191, China, email: dai5188@hotmail.com (Y. Dai)*
[b]*Laboratory of Environmental Remediation,College of Resources and Environment, Northeast Agricultural University, No. 600 Changjiang Road, Xiangfang District,Harbin 150030, China, Tel./Fax: +8645155190825; emails: zhihua-liu@neau.edu.cn (Z. Liu), 982464423@qq.com (Y. Sun), 67384708@qq.com (J. Li), 809424378@qq.com (S. Li), achilles.wy@foxmail.com (W. Yue)*
[c]*Research Center for Eco-Environmental Sciences,Chinese Academy of Sciences, NO.18, Shuang Qing Road, Haidian District, Beijing 100085, China, email: 2090378492@qq.com (M. Liu)*
[d]*College of Environmental Science and Engineering, Tongji University, No.1239 Siping road, Yangpu District, Shanghai 200092, China, email: 495761231@qq.com (Y. Jiang)*

Received 24 July 2018; Accepted 21 January 2019

**ABSTRACT**

The use of biochar prepared from waste crop straw for the removal of tetracycline (TC) in water has a profound influence on the protection of agricultural water environment. In this study, biochar (BC) was prepared from waste corn straw and wheat straw. The adsorption experiments were carried out on few factors: adsorption time, BC dosages, pH and ionic strength. The results showed that the adsorption of TC by BC derived from corn (C-BC) and BC derived from wheat (W-BC) fitted to the Langmuir model. The equilibrium time for adsorption of C-BC and W-BC was 60 min, the optimal amount of BCs dose was 10 $g \cdot L^{-1}$. The maximum saturated adsorption of TC by C-BC and W-BC were 49.56 and 42.12 $mg \cdot g^{-1}$, respectively. The presence of $Mg^{2+}$ hindered the adsorption of TC by BCs. The adsorption mechanism was analyzed from the perspective of adsorption kinetics, and both BCs were chemical adsorption. Research showed that biochar in the northeast is cheap and easy to obtain, and the adsorption efficiency was high. Therefore, the use of BC which prepared from corn straw and wheat straw to removal TC has broad prospect.

*Keywords:* Adsorption mechanism; Crop waste; Maximum adsorption capacity; Thermodynamic analyses

## 1. Introduction

Tetracycline (TC) is an antibiotic with multi-resistance to bacteria including gram-negative and gram-positive bacteria [1]. TC in environment originates from industrial and medical wastes as well as wastewater coming from livestock and poultry farming [2]. In 2009, the amount of TC used in the U.S. aqua cultural industry was 4,611.892 ton, which accounted for 35.3% of all antibiotic usage [3]. The EU consumes approximately 5,000 tons of antibiotics each year, in which the use of TC amounts to 2,300–2,600 ton [4], accounting for 46%–52% of the total. As the largest one in production and use of TC antibiotics [5], in 2013, China used TC antibiotics about 12,000 ton, which were 11 times more than the total use of antibiotics by Britain [6]. It is difficult to absorb or degrade TC by organisms even it is excreted from the body that TC remains biological active. Seriously, TC may even induce mutation of microorganism through

* Corresponding author.

induction and generate resistance genes. So, TC poses a certain threat to the ecological environment as well as human health. Finding an efficient TC removal method has become an urgent problem [7].

Adsorption is a common method to remove TC in water environment, by its low cost and without secondary pollution [8,9]. There are a lot of materials to absorb TC, such as montmorillonite [10]; kaolinite [11]; chitosan [12]; magnetic composites derived from bagasse [13]; Alkaline biochar (BC) [14]; magnetic microspheres-NDA150 [15]; multi-walled carbon nanotubes [16]; A-MCM-41 [17] and so on. Compared with those adsorbents, BC have the pretty adsorption properties due to its complicated pore structure and large specific surface area. Hence, this work utilized BC derived from waste crop straw and wheat straw to remove TC.

Agriculture occupied the most production in Heilongjiang Province, China, so, there is a lot of crop straw each year. In 2014, the straw resources (dry weight) of Heilongjiang Province totaled more than 90 million ton. Traditionally, the use of crop straw in Heilongjiang Province included about three methods, animal husbandry feed, burn or rot in the field, and energy resource. For animal husbandry feed, it was accounted for about 30% (mainly corn and soybean straw). It's burned or rotted in the field and account for about 30%. And, it's about 30% to use for the energy use of cooking fuel for rural households. Another 10% is used for returning straw, industrial material and edible fungi base material, etc. [18]. BC has been widely used to remove pollutants in water because of its high density of micropore structure, large specific surface area and high adsorption capacity [19]. However, there are few reports about the use of BC to remove TC from water. In this study, TC, a typical antibiotic, was used as the adsorbate, and two kinds of BC that derived from corn and wheat straw (C-BC and W-BC), were used as adsorbents. The adsorption performance of two BCs on TC was compared. In this study, physical-chemical properties of C-BC and W-BC were studied by single factor analysis. The three factors that adsorbent dosage, adsorption time and concentration of ion on the adsorption test were studied. In this work, on the basis of studying the adsorption characteristics of adsorbents on TC in water, the adsorbent regeneration technology was added, which provided the necessary reference for practical industrial application in the future.

## 2. Materials and methods

### 2.1. Materials

TC standard product (purity 97.5%) was purchased from Shanghai Haring Biotechnology Co., Ltd. $MgCl_2$ was purchased from Tianjin Guangfu Fine Chemicals Institute for pure analysis. Deionized water was used in all the experiments. C-BC and W-BC were provided by the Biochar Engineering and Technology Research Center of Liaoning Province, Shenyang Agricultural University, China. After dried, the C-BC and the W-BC was ground to pass the 0.425 mm standard sieve, sprayed with gold and examined for specific surface area. The basic characteristics of C-BC and W-BC are shown in Table 1.

Table 1 Basic characteristics of corn biochar (C-BC) and wheat biochar (W-BC)

| | C-BC | W-BC |
|---|---|---|
| Superficial area | | |
| Total surface area ($m^2 \cdot g^{-1}$) | 151 | 127 |
| Micropore surface area($m^2 \cdot g^{-1}$) | 62 | 51 |
| Mesoporous surface area and macroporous surface area($m^2 \cdot g^{-1}$) | 89 | 76 |
| Equal charge point($pH_{PZC}$) | 5.8 | 4.5 |

### 2.2. Physic-chemical properties

Low-vacuum scanning electron microscope (SEM) (JSM-6360LA) was used to observe the surface structure of C-BC and W-BC. The study of X-ray diffraction (XRD) was performed by an X-ray Diffractometer 1730 (Philips Ltd. Amsterdam, Netherlands) using Cu K$\alpha$ radiation.

The specific surface area detection (BET) was used to determine the specific surface area of C-BC and W-BC. The determination method was as follows: C-BC and W-BC of 50 mg were separately dried overnight. After degassing under $N_2$ protection, the $N_2$ sorption isotherm was measured in a nitrogen bath (–196°C), and then the specific surface area of C-BC and W-BC was calculated using the BET formula Eq. (1) [20]. The pore parameters of the BET analysis (Autosorb 6AG, Yuasa lonics Co., Osaka, Japan) were obtained by physical adsorption analysis of nitrogen gas by a gas adsorption instrument.

$$S_{BET} = A_m N_A V_m / 22414 \quad (1)$$

where $S_{BET}$ meant the specific surface area of the sample; $A_m$ meant the average cross-sectional area of a single adsorbed molecule; $N_A$ meant the Avogadro constant, which is $6.02 \times 10^{23}$; $V_m$ meant the saturated adsorption amount when the surface is covered with a monolayer with the unit of $mL \cdot g^{-1}$.

The zero charge point ($pH_{pzc}$) of the adsorbents (C-BC and W-BC) was determined by the pH drift method [21]. An aliquot (50 mL) of 0.01 M NaCl solution was added to a series of flasks. NaOH (0.1–1.0 M) or HCl (0.1–1.0 M) was used to adjusted the initial pH ($pH_i$) from 1.98 to 13.25. 0.1 g of C-BC and W-BC samples were added to each flask and then shaked for 48 h. Then, the final pH ($pH_f$) of the mixture was measured. The $pH_{pzc}$ is defined as the point determined by $pH_f$–$pH_i$ passing through the point of the axis $pH_i = pH_f$ [22].

### 2.3. Adsorption kinetics

In this experiment, the initial concentration of TC was 27.78 $mg \cdot L^{-1}$ which was set from 25 to 30 $mg \cdot L^{-1}$ and shaken at 23°C and pH 7.0. Samples were taken at 10 min, 20 min, 30 min, 45 min, 1 h, 2 h, 4 h, and 6 h of the adsorption reaction, respectively. After the supernatant was filtered, the TC content in the supernanant was measured using the UV spectrophotometer (V-550, Shimadzu, Japan) at the wavelength of 358 nm.

*2.4. Batch adsorption experiments: adsorbents dosages and ion concentration*

C-BC and W-BC with different amount of 25, 50, 75, 100, 150, 200, 250, and 300 mg was added, respectively, into 100 mL flasks with 25 mL TC solution. The initial concentration of TC was 27.78 mg·L$^{-1}$. The samples were shaken at 23°C and pH 7.0 in dark. After 12 h, samples were taken out. After the supernatant was filtered, the TC content in the supernanant was measured using the UV spectrophotometer (V-550, Shimadzu, Japan).

C-BC and W-BC with the amount of 100 mg was added in a 100 mL flask with 25 mL of TC solution. Accurate amounts of 0, 0.01, 0.05 and 0.1 moL·L$^{-1}$ $MgCl_2$ solutions were added to the respective conical flasks. The initial concentration of TC was 27.78 mg·L$^{-1}$. The samples were shaken at 23°C and pH 7.0.

## 3. Results and discussion

*3.1. Physical and chemical characteristics*

The scanning electron microscopy was carried out in order to visually examine the surface pore structure of C-BC and W-BC. The results are shown in Figs. 1 and 2. Fig. 1 shows that there is uneven distribution of pores and a large number of irregular raised structures on the rough surfaces of C-BC. Fig. 2 shows that compared with the structure of C-BC, the W-BC had a finer surface and more abundant pores. Both have a large number of raised structures, increasing the specific surface area.

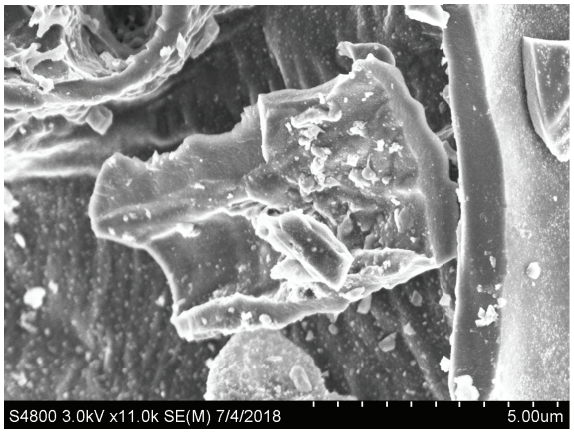


Fig. 1. SEM image of C-BC.

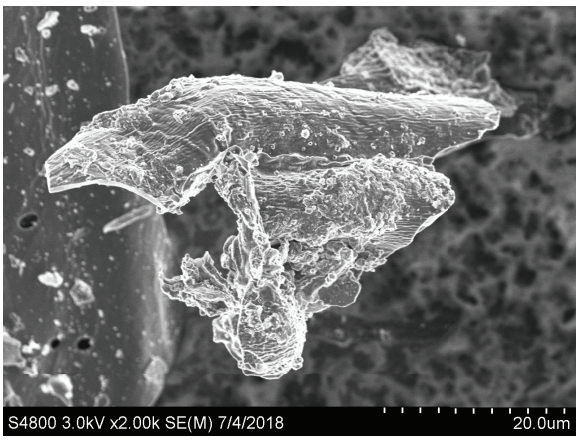


Fig. 2. SEM image of W-BC.

The crystal structure and phase composition characteristics can be analyzed by XRD images. XRD intensity patterns of C-BC and W-BC are shown in Figs. 3 and 4. As shown in Fig. 3, the pattern of the C-BC shows the formation of the main peak intensity at 2θ = 23.8°. The peak around at 2θ = 16° to 2θ = 30° indicated that because of the pyrolysis at 600°C, the BC deformed grapheme like atomic structure [23]. As shown in Fig. 4, the image of the W-BC showed that the major peak intensity was at 2θ = 27.2°. The sharp peaks of W-BC suggested the presence of crystallinity in the W-BC phases [24].

*3.2. Effect of adsorption time*

Equilibrium time, one of the most important parameters, determine the capacity of adsorbents that used. The adsorption rate of the adsorbent is inversely proportional to

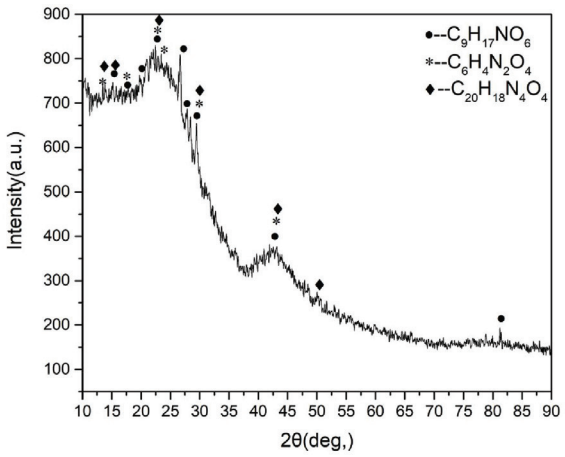


Fig. 3. XRD patterns of C-BC.

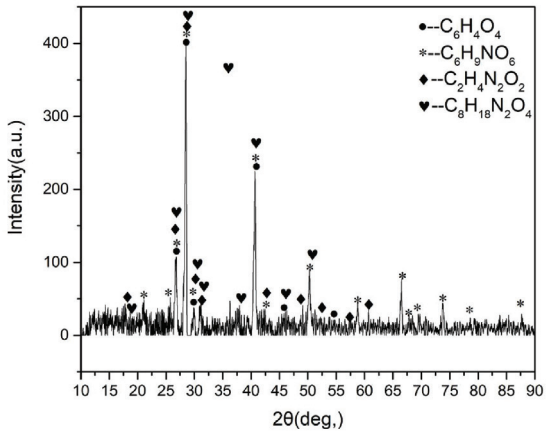


Fig. 4. XRD patterns of W-BC.

the equilibrium time. The adsorption rate of the adsorbent is related to many indicators such as microporous structure, the amount of adsorbent dosages, the adsorption time, the initial concentration of the adsorbent, the pH of solution and the ion concentration in the solution. The experiment should determine the adsorption equilibrium time at first. As shown in Fig. 5, the reaction quickly reached equilibrium at 60 min. In the initial stage the removal ratio was high because of there were high concentration of TC and numerous adsorption sites of BC [22]. And the adsorption sites were gradually occupied by TC, the adsorption ratio gradually decreased as time went on, eventually reached the adsorption equilibrium. The removal of TC by C-BC and W-BC when the adsorption equilibrium were 81.44% and 77.10%, respectively.

### 3.3. Adsorption kinetics

The adsorption kinetics could help to analysis the adsorption mechanisms. Two kinds of kinetic models, as pseudo-first-order kinetic model and pseudo-second-order kinetic model, were carried out [22]. The kinetic rate equation can be expressed as Eq. (2).

$$dq_t/dt = \left(q_e - q_t\right)^n \tag{2}$$

where $q_e$ and $q_t$ correspond to the adsorption capacity of adsorbents per unit mass (mg·g$^{-1}$) at equilibrium and at time $t$, respectively. And $k_n$ is the rate constant of $n$ adsorptions ($k_n$ units min$^{-1}$, $n$ = 1; g·mg$^{-1}$·min, $n$ = 2). The linear integral form of the kinetic rate equation is as follows:

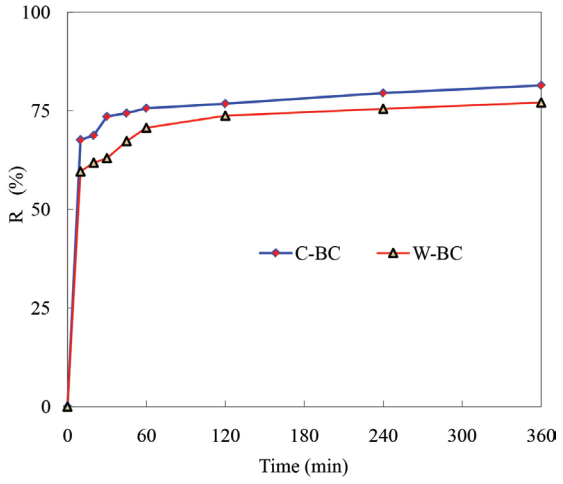


Fig. 5. Effect of adsorption time of TC by the C-BC and W-BC (initial concentration of TC (27.78 mg·L$^{-1}$), pH 7.0, at 23°C).

Pseudo-first-order kinetic Eq. (3) ($n$ = 1) is:

$$\ln\left(q_e - q_t\right) = \ln q_e - k_1 t \tag{3}$$

Pseudo-second-order kinetic Eq. (4) ($n$ = 2) is:

$$t/q_t = 1/(k_2 q_e^{\,2}) + t/q_e \tag{4}$$

The best model is selected based on the correlation coefficients ($R^2$) and the value of $q_e$. The pseudo-first-order model and the pseudo-second-order model were used to fit the kinetic experimental data to explain the kinetics of TC removal. The results were shown in Table 2. The results indicated that the pseudo-second-order kinetic model were greater fitted to the adsorption of TC on BCs by comparing the correlation coefficients [25]. The adsorption capacity (calculated $q_e$) was calculated by the pseudo-second-order kinetic equation, indicated that the adsorption processes of TC by the two kinds of BC were greater fitted with the pseudo-second-order kinetic model. The two models could indicate the surface diffusion, surface adsorption and intragranular diffusion processes of the adsorption reaction. The results showed that the adsorption processes of TC on BCs were mainly chemical adsorption. Therefore, the adsorption processes could quickly reached adsorption equilibrium, which is consistent with the adsorption equilibrium time.

### 3.4. Effect of adsorbent dosages

The effects of the adsorbent dosages on the adsorption ratio of TC are shown in Fig. 6. With the increased of the amount of adsorbent, the adsorption ratio of TC rapidly increased at first and then slowly increased. When the dosages of BC increased from 0 to 10 g·L$^{-1}$, the removal of TC increased rapidly. When the C-BC and W-BC amounted to 10 g·L$^{-1}$, the removal ratio of TC has reached 81.44% and 77.10%, respectively. However, when the dosages of C-BC and W-BC reached 12 g·L$^{-1}$, the removal ratio of TC reached 84.56 % and 81.27%, respectively. And there were still accessible adsorbent sites [22]. And the removal ratio of TC is gradually increased after the addition of adsorbent to a certain extent. Therefore, 10 g·L$^{-1}$ of BCs were added into after experiments in this work.

### 3.5. Effect of pH

As well known, pH is a vital factor to the adsorption in the aqueous solution [26].We used 0.1–1 mol/L HCl or NaOH were used to adjust the initial pH of solution from

Table 2
Parameters of pseudo-first-order and pseudo-second-order kinetics models for TC

| Samples | Pseudo-first-order model | | | Pseudo-second-order model | | | Experience |
|---|---|---|---|---|---|---|---|
| | $k_1$(min$^{-1}$) | Calculated $q_e$ (mg·g$^{-1}$) | $R^2$ | $k_2$ (g·mg$^{-1}$·min$^{-1}$) | Calculated $q_e$ (mg·g$^{-1}$) | $R^2$ | $q_e$ (mg·g$^{-1}$) |
| C-BC | 0.0078 | 3.06 | 0.9149 | 0.0457 | 49.98 | 0.9997 | 49.56 |
| W-BC | 0.0106 | 2.18 | 0.9333 | 0.0236 | 43.25 | 0.9998 | 42.12 |

3 to 11 to detect the removal change. The removal ratio of TC adsorption by C-BC and W-BC is shown in Fig. 7. With the increase of pH, the removal ratio of BCs reduced. When pH changed from 3 to 11, the removal ratio of C-BC changed from 89.56% to 72.51% while the removal ratio of W-BC varied from 86.54% to 70.13%. Under higher pH, the adsorption of TC by BCs was more intense hindered. This may be due to the higher pH, hydrogen bonds between the TC and BCs reduced, resulting in lower removal ratio [27].

### 3.6. Effect of ionic strength

The effect of ionic strength of $MgCl_2$ ($Mg^{2+}$) on the removal of TC was shown in Fig. 8 [28]. The removal capacity of TC by C-BC and W-BC decreased with the ion concentration of $MgCl_2$ in solution increasing. When the concentration of $MgCl_2$ was 0, 0.01, 0.05 and 0.10 mol·L$^{-1}$, the removal ratio of TC by C-BC was from 70.73% to 81.44%. The removal ratio of TC by W-BC was from 64.27% to 77.1%. With the increase of ionic strength, TC usually accompanied by an increase in the distribution of adsorbents ever, as the ionic strength increased, the amount of TC adsorbed by BCs decreased. Since the $pH_{pzc}$ value of C-BC was 5.8 and the $pH_{pzc}$ value of W-BC was 4.5, the surface of both BCs was mainly negatively charged at the experimental pH of 7.0. Through electrostatic interaction, $Mg^{2+}$ was favorably adsorbed on C-BC and W-BC [29]. It had been speculated that $MgCl_2$ was superior to the strongest sites in both BCs and competes with the two BCs in space. Due to surface heterogeneity, TC adsorption decreased.

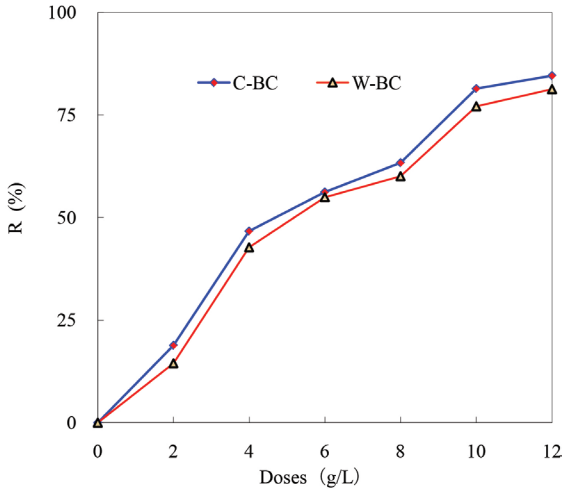


Fig. 6. Effect of adsorbent dosage on TC removal ratio (initial concentration of TC (27.78mg·L$^{-1}$), pH 7.0, at 23°C).

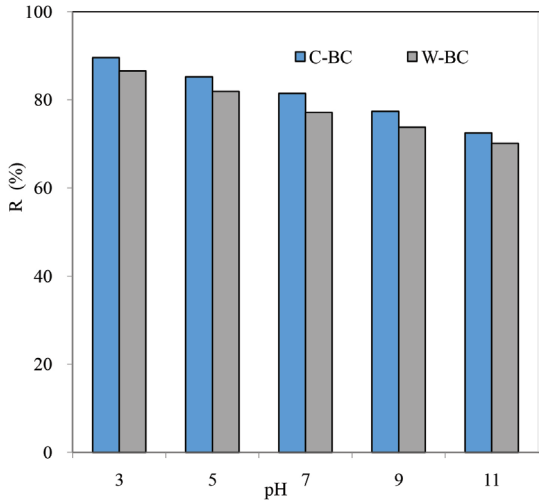


Fig. 7. Effect of pH on the adsorption of TC by the C-BC and W-BC (initial concentration of TC (27.78 mg·L$^{-1}$) at 23°C).

### 3.7. Adsorption isotherm

As shown in Fig. 9, the adsorption isotherms of TC were a typical Langmuir-type and Freundlich-type curves. The reciprocal of the amount of TC adsorbed to BC had a linear correlation with the inverse of the equilibrium concentration of TC in the solution. It is summarized in Table 2 that the parameters of Eqs. (5) and (6) based on the adsorption isotherms of BC [25].

Langmuir Eq. (5):

$$q_e = Q_0 K_L C_e / \left(1 + K_L C_e\right) \tag{5}$$

Among them, $q_e$ (mg·g$^{-1}$) means the amount of adsorption; $Q_0$ (mg·g$^{-1}$) represents the saturated adsorption amount; $K_L$ (L·mg$^{-1}$) is the adsorption equilibrium constant of Langmuir isotherm; $C_e$ (mg·L$^{-1}$) is the concentration of TC when the time at adsorption equilibrium. The equation for the adsorption of TC $q_e$ (mg·g$^{-1}$) $q_e = (C_0 - C_e) \times (V/m)$, $C_0$ (mg·L$^{-1}$) and $V$ (L) are the initial concentrations of TC in solution and the volume of solution, respectively, $m$ (g) is the mass of the sample.

Freundlich Eq. (6):

$$q_e = K_F C_e^{1/n} \tag{6}$$

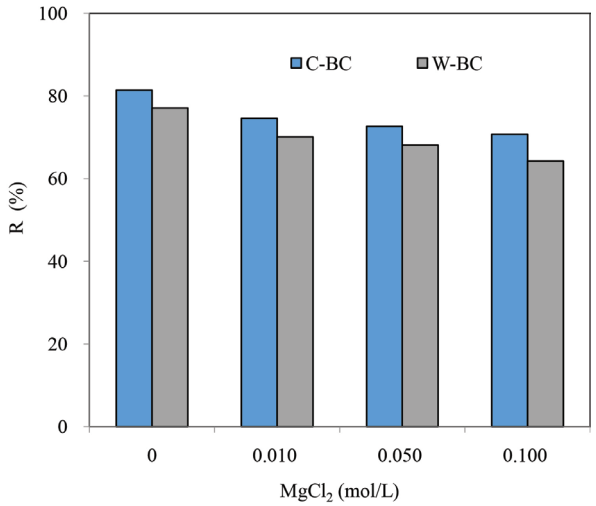


Fig. 8. Effect of ionic strength on the adsorption of TC by the C-BC and W-BC (initial concentration of TC (27.78 mg·L$^{-1}$), pH 7.0, at 23°C).

Among them, $K_F$ (L·mg$^{-1}$) is a parameter of the adsorption capacity with the Freundlich model; the constant $n$ is an empirical parameter related to the adsorption strength of the adsorbent. When the $1/n$ value is in the range of 0.1 to 0.5, the adsorption process is favored [25]. For comparison, the Freundlich constant is calculated in the same way as Langmuir.

The adsorption isotherms of TC on BC were respectively fitted to Langmuir model and Freundlich model (Table 2). The experimental data were more fitted to Langmuir model, indicated that the adsorption of TC by BCs were mainly based on uniform adsorption. The various adsorption sites on the BC surface were equal to TC energy.

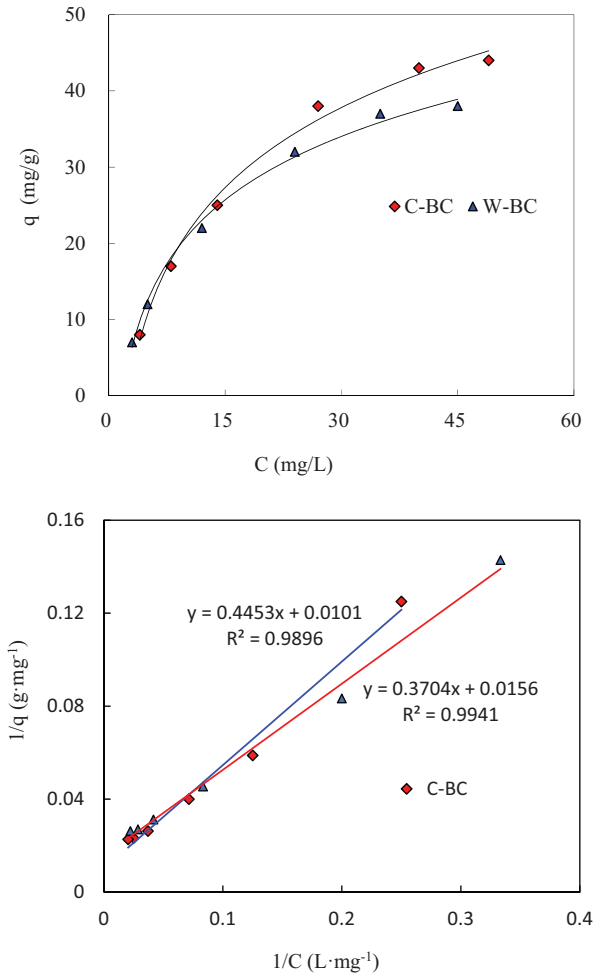


Fig. 9. Adsorption isothermal curve of TC by the C-BC and W-BC (initial concentration of TC 10–100 mg·L$^{-1}$), pH 7.0, at 23°C).

Table 3 shows the parameters of BC obtained from the Langmuir adsorption isotherm: $Q_0$ of C-BC and W-BC are 49.56 and 42.12 g·mg$^{-1}$; $K_L$ of C-BC and W-BC are 0.0227 and 0.0421 L·mg$^{-1}$, respectively. The above results indicated that the saturated adsorption capacity of BCs had difference between C-BC (142 m$^2$·g$^{-1}$) and W-BC (127 m$^2$·g$^{-1}$). There was no significant difference in specific surface area, indicated that the specific surface area played a major role. Adsorption of these two BCs were superior through compared with adsorbents reported in the literature (kaolinite (4.3 mg·g$^{-1}$); chitosan (13.3 mg·g$^{-1}$); magnetic composites derived from bagasse (48.4 mg·g$^{-1}$); alkaline BC (58.8 mg·g$^{-1}$)) [11–14] in Table 4.

### 3.8. Thermodynamic analyzes

The study of thermodynamic indicators of adsorption processes were carried out. $\Delta G°$ is the standard free energy change (kJ·mol$^{-1}$), $\Delta H°$ is the standard enthalpy (kJ·mol$^{-1}$), and $\Delta S°$ is the standard entropy (J·mol$^{-1}$·K$^{-1}$). Use the following Eqs. (7) and (8) to determine thermodynamic parameters [22]:

$$\Delta G^{\circ} = -RT\ln\left(C_{ad.e}/C_e\right) \tag{7}$$

$$\ln\left(C_{ad.e}/C_e\right) = \Delta S^{\circ}/R - \Delta H^{\circ}/RT \tag{8}$$

Among them, $R$ is the ideal gas constant (8.314 J·mol$^{-1}$·K$^{-1}$); $T$ is the Kelvin temperature. $C_{ad.e}$ and $C_e$ correspond to the equilibrium concentration of TC (mg·L$^{-1}$) on the C-BC and W-BC and solution, respectively. Determine the values of $\Delta H°$ and $\Delta S°$ based on the slope and intercept of the van Hoff plot ($InC_{ad.e}/C_e$ vs. $1/T$), respectively.

Table 5 shows that the $\Delta G°$ of C-BC was –9.37 kJ·mol$^{-1}$, and the $\Delta G°$ of W-BC was –7.68 kJ·mol$^{-1}$. Since both $\Delta G°$ were negative, C-BC and W-BC had feasibility and spontaneity to adsorb TC. The adsorption process of both adsorbents was endothermic. $\Delta S°$ was a positive value (24.87 kJ·mol$^{-1}$ and 31.46 kJ·mol$^{-1}$), indicated that the adsorbent had an increased affinity for TC due to an increase in randomness between the interface and the solid phases [30].

### 3.9. Adsorption mechanism

The mechanism of the adsorption for TC of C-BC and W-BC maybe controlled by multi-mechanisms. The pore-filling was a physical adsorption that might play a leading role in the adsorption of TC on C-BC and W-BC.

Table 3
Parameters of TC adsorption isotherms fitted with Langmuir and Freundlich models

| Samples | Langmuir model | | | Freundlich model | | |
|---|---|---|---|---|---|---|
| | $Q_0$ (mg·g$^{-1}$) | $K_L$ (L·mg$^{-1}$) | $R^2$ | $K_F$ (L·mg$^{-1}$) | $1/n$ | $R^2$ |
| C-BC | 49.56 | 0.0227 | 0.9896 | 3.7485 | 0.6705 | 0.9582 |
| W-BC | 42.12 | 0.0421 | 0.9941 | 4.0900 | 0.6219 | 0.9699 |

Table 4
Maximum uptake capacity for the adsorption of TC onto various adsorbents

| Adsorbents | $Q_0$ of TC | References |
|---|---|---|
| Kaolinite | 4.30 | [11] |
| Chitosan | 13.30 | [12] |
| W-BC | 42.12 | This study |
| C-BC | 49.56 | |
| Magnetic composites derived from bagasse | 48.40 | [13] |
| Alkaline BC | 58.8 | [14] |

Table 5
Thermodynamic parameters of TC adsorption

| Samples | $T$ (K) | $\Delta G°$ (kJ·mol$^{-1}$) | $\Delta H°$ (kJ·mol$^{-1}$) | $\Delta S°$ (J·mol$^{-1}$·K$^{-1}$) |
|---|---|---|---|---|
| C-BC | 296 | –9.37 | 11.23 | 24.87 |
| W-BC | 296 | –7.68 | 13.56 | 31.46 |

The surface area of C-BC was higher than that of W-BC (Table 1), which gave C-BC a higher adsorption capacity for TC, confirming the pore-filling effect [24]. According to precious study which has been reported, TC species sizes are smaller than 1.27 nm, when the pore size of the adsorbent is about twice times bigger than the size of the pollutant particles, the adsorbent has greater adsorption capacity, which suggesting that it is reasonable to expect that the micropore could be suitable for TC adsorption with sufficient pore size to allow penetration of TC into pores. As shown in Table 1, the micropore surface area of C-BC is richer than that of W-BC, which is further proof this view. However, this is not the only mechanism.

According to the previously reported results, the adsorption mechanism of BC materials on TC mainly involved not only pore-filling but also π-π EDA and electrostatic attraction [32]. Due to the functional groups of TC, TC could undergo many electronic coupling interactions, which including π-π EDA, Lewis acid-base and electrostatic interactions [31]. Because of the electron with drawing ability of the ketone group, the properties of π acceptor in TC were influenced by the conjugated enone structure. The function groups of TC structure have a strong electron-accepting ability, and the benzene ring of TC is a π-electron acceptor. Therefore, an aromatic hydrocarbon ring can be supplied to the surface of the BC to form a specific π-π EDA interaction [32]. Many studies of adsorption on TC have carried out this conclusion. Therefore, π-π EDA is one of the main mechanisms of C-BC and W-BC adsorption of TC as well as electrostatic force. In addition, there will form H-bonding between the phenol, amine, hydroxyl and enone moieries of TC and hydroxyl functional groups on the surface of C-BC and W-BC [33].

## 4. Conclusions

This study measured the adsorption capacity of C-BC and W-BC on TC. The effects of adsorption time, dosages of adsorbents and ionic strength ($MgCl_2$) on adsorption of C-BC and W-BC were studied. It was found that the adsorption of C-BC and W-BC had a fast adsorption process to TC. The adsorption rate was fast at the initial stage and the adsorption capacity was great. With the progress of the reaction, the TC concentration decreased and the reaction ratio gradually slowed down. When the reaction reached 60 min, most of the TC in the solution had been adsorbed and reached adsorption equilibrium. Simultaneous addition of $MgCl_2$ inhibited the adsorption of TC on C-BC and W-BC, but its inhibition was limited. The adsorption of TC by C-BC and W-BC could be well fitted to Langmuir isotherm model. The maximum saturated adsorption capacity of TC by C-BC and W-BC were 49.56 and 42.12 mg·g$^{-1}$, respectively. Studies have shown that in the northeastern region, because of the cheap and readily available BC, the adsorption effect was significant. Therefore, the removal of TC from water by BC has broad prospects, and the mechanism of the adsorption for TC of C-BC and W-BC maybe controlled by muti-mechanisms that included pore-filling effect and π-π EDA.

## Acknowledgments

This work was supported by Key Laboratory of Original Agro-Environmental Pollution Prevention and Control, Ministry of Agriculture/Tianjin Key Laboratory of Agro-environment and Safe-product (16nybcdhj-2). This work was also supported by National Natural Science Foundation of China (41301316) and National Key Technologies R & D Program of China (2018YFD0300103-4-2) to Dr. Liu.

## References

[1] L. Yan, D.Q. Fan, X.X. Jiang, X.N. Jim, H.H. Yang, S.Q. Li, M. Yu, Adsorption behaviour of tetracycline antibiotics in black soil and albic soil, J. Northeast. Agric. Univ., 48 (2017) 54–62.
[2] Q.Y. Xie, T. Li, Z.L. Wang, H.M. Dong, W.S. Guo, G.S. Gao, B.C. Jiang, H.S. Wang, G.Q. Xu, Study on the kinetics of metabolism of tetracycline in horses, J. Northeast. Agric. Univ., 4 (1983) 22–26.
[3] US Food, Drug Administration. Summary report on antimicrobials sold or distributed for use in food-producing animals, 2010.
[4] R. Hirsch, T. Ternes, K. Haberer, K.L. Kratz, Occurrence of antibiotics in the aquatic environment, Sci. Total Environ., 225 (1999) 109–118.
[5] G. Sun, S.W. Xu, Investigation and resistance analysis of campylobacter jejuni in broiler, J. Northeast. Agric. Univ., 46 (2015) 64–68.
[6] Q.Q. Zhang, G.G. Ying, C.G. Pan, Y.S. Liu, J.L. Zhao, Comprehensive evaluation of antibiotics emission and fate in the river basins of China: source analysis, multimedia modeling, and linkage to bacterial resistance, Environ. Sci. Technol., 49 (2015) 6772–6782.
[7] S. Rodriguez-Mozaz, S. Chamorro, E. Marti, B. Huerta, M. Gros, A. Sànchez-Melsió, C.M. Borrego, D. Barceló, J.L. Balcázar, Occurrence of antibiotics and antibiotic resistance genes in hospital and urban wastewaters and their impact on the receiving river, Water. Res., 69 (2015) 234–242.
[8] P.H. Chang, J.S. Jean, W.T. Jiang, Z. Li, Mechanism of tetracycline sorption on rectorite, Colloids. Surf., A., 339 (2009) 94–99.
[9] P.H. Chang, Z.H. Li, T.L. Yu, S. Munkhbayer, T.H. Kuo, Y.C. Hung, J.S. Jean, K.H. Lin, Sorptive removal of tetracycline from water by palygorskite, J. Hazard. Mater., 165 (2009) 148–155.
[10] M.E. Parolo, M.C. Savini, J.M. Valles, M.T. Baschini, M.J. Avena, Tetracycline adsorption on montmorillonite: pH and ionic strength effects, Appl. Clay. Sci., 40 (2008) 179–186.

[11] Z. Li, L. Schulz, C. Ackley, N. Fenske, Adsorption of tetracycline on kaolinite with pH-dependent surface charges, J. Colloid. Interface. Sci., 351 (2010) 254–260.
[12] J. Kang, H.J. Liu, Y.M. Zheng, J.H. Qu, J.P.Chen, Systematic study of synergistic and antagonistic effects on adsorption of tetracycline and copper onto a chitosan, J. Colloid. Interface. Sci., 344 (2010) 117–125.
[13] N. Rattanachueskul, A. Saning, S. Kaowphong, N. Chumha, L. Chuenchom, Magnetic carbon composites with a hierarchical structure for adsorption of tetracycline, prepared from sugarcane bagasse via hydrothermal carbonization coupled with simple heat treatment process, Bioresour. Technol., 226 (2017) 164–172.
[14] P. Liu, W. Liu, H. Jiang, J. Chen, W. Li, H. Yu, Modification of biochar derived from fast pyrolysis of biomass and its application in removal of tetracycline from aqueous solution, Bioresour. Technol., 121 (2012) 235–240.
[15] Q. Zhou, Z. Li, C. Shuang, A. Li, M. Zhang, M. Wang, Efficient removal of tetracycline by reusable magnetic microspheres with a high surface area, Chem. Eng. J., 210 (2012) 350–356.
[16] L. Zhang, X. Song, X. Liu, L. Yang, F. Pan, J. Lv, Studies on the removal of tetracycline by multi-walled carbon nanotubes, Chem. Eng. J., 178 (2011) 26–33.
[17] M. Liu, L. Hou, S. Yu, B. Xi, Y. Zhao, X. Xia, MCM-41 impregnated with a zeolite precursor, synthesis, characterization and tetracycline antibiotics removal from aqueous solution, Chem. Eng. J., 223 (2013) 678–687.
[18] Y.F. Huang, Practice and consideration of comprehensive utilization of straw in Heilongjiang Province, China Financ. Econo. News, 2015-03-26.
[19] L. Yan, M. Yum, J.X. Zhang, S.Q. Li, L.Y. Hou, Z.W. Qin, Effect of three fungicides on diversity of soil bacterial community, J. Northeast. Agric. Univ., 44 (2013) 29–33.
[20] W.Q. Zhu, D.Z. Tang, Y.X. Yu, L. Wang, Shale nitrogen adsorption BET specific surface area measurement error correction method, Sci. Technol. Eng., 29 (2015) 1671–1815.
[21] Y.S. Al-Degs, M.I. El-Barghouthi, A.H. El-Sheikh, G.M. Walker, Effect of solution pH, ionic strength, and temperature on adsorption behavior of reactive dyes on activated carbon, Dyes. Pigm., 77 (2008) 16–23.
[22] Y.J. Dai, D.F. Zhang, K.X. Zhang, Nitrobenzene-adsorption capacity of NaOH-modified spent coffee ground from aqueous solution, J. Taiwan. Inst. Chem. Eng., 68 (2016) 232–238.
[23] P. Devi, A.K. Saroha, Synthesis of the magnetic biochar composites for use as an adsorbent for the removal of pentachlorophenol from the effluent, Bioresour. Technol., 368 (2012) 420–426.
[24] H.X. Zhao, Y.H. Lang, Adsorption behaviors and mechanisms of florfenicol by magnetic functionalized biochar and reed biochar, J. Taiwan. Inst. Chem. Eng., 8 (2018) 152–160.
[25] H.M. Jang, S. Yoo, Y.K. Choi, S. Park, E. Kan, Adsorption isotherm, kinetic modeling and mechanism of tetracycline on Pinus taeda-derived activated biochar, Bioresour. Technol., 259 (2018) 24–31.
[26] Y.N. Yang, Y. Chun, G.Y. Sheng, M. Huang, pH-dependence of pesticide adsorption by wheat-residue-derived black carbon, Langmuir, 20 (2004) 6736–6741.
[27] N. Wang, Y.W. Hou, J.J. Peng, J.L. Dai, C. Cai, Research progress on adsorption of organic pollutants by biochar, Environ. Chem., 31 (2012) 287–295.
[28] S.V. Novais, M.D.O., Zenero, J., Tronto, R.F., Conz, C.E.P., Cerri, Poultry manure and sugarcane straw biochars modified with $MgCl_2$ for phosphorus adsorption, J. Environ. Manage., 214 (2018) 36–44.
[29] M.M. Rao, A. Ramesh, G.P. Rao, K. Seshaiah, Removal of copper and cadmium from the aqueous solutions by activated carbon derived from ceiba petandra hulls, J. Hazard. Mater., 129 (2006) 123–129.
[30] Z. Al-Qodah, W.K. Lafi, Z. Al-Anber, M. Al-Shannag, A. Harahsheh, Adsorption of methylene blue by acid and heat treated diatomaceous silica, Desalination, 217 (2007) 212–224.
[31] P. Peng, Y.H. Lang, X.M. Wang, Adsorption behavior and mechanism of pentachlorophenol on reed biochars: pH effect, pyrolysis temperature, hydrochloric acid treatment and isotherms, Ecol. Eng., 90 (2016) 225–233.
[32] L. Ji, W. Chen, L. Duan, D. Zhu, Mechanisms for strong adsorption of tetracycline to carbon nanotubes: a comparative study using activated carbon and graphite as adsorbents, Environ. Sci. Technol., 43 (2009) 2322–2327.
[33] G. Zhang, X. Liu, K. Sun, F. He, Y. Zhao, C. Lin, Competitive sorption of metsulfuron-methyl and tetracycline on corn straw biochars, J. Environ. Qual., 41 (2012) 1906–1915.